ORIGINAL ARTICLE

Numerical simulation and experimental research on rubber flexible-die forming limitation with new position-limited backpressure mechanism

Zhiren Han[1] (iD) · Chuang Wei[1] · Simin Du[1] · Zhen Jia[1] · Xinyang Du[1]

Abstract

The forming limitation and the wall thickness distributions are the two main parameters for estimating the forming quality of T-shaped tubes. In this paper, the effects of three key factors on the forming limitation and the wall thickness distributions are investigated, which are punch front distance l_1, reverse height h_1, and the matching relationship between rubber hardness and axial feed Δl. A new position-limited backpressure mechanism is proposed, which is made up of the rigid position-limited lever, the flexible backpressure medium, and the rigid spacer. The simulations and experiments are carried out. Both results show that the thinning rate of the wall thickness decreases first and then increases, and the thickening rate decreases gradually with the increase of l_1. The branch reaches the highest with the l_1 of 5mm under the requirements of thinning rate and thickening rate. With the rise of reverse height h_1, the bigger h_1 is beneficial to the wall thickness thinning suppress at the top of the branch, and the branch reached the highest when h_1 is 7mm. When Δl is fixed, the rubber hardness has a significant influence on the forming defects. The exorbitant rubber hardness causes the branch to rupture, and the excessive axial feed causes the wall to wrinkle. When rubber hardness is fixed, the thickening rate decreases with the increase of Δl. The best forming limitation and thickness distribution are achieved with the punch front distance l_1 of 5mm, the reverse height h_1 of 7mm, the rubber hardness of 75HA, and the axial feed Δl of 24mm.

Keywords T-shaped tube forming · Rubber flexible-die forming · Position-limited backpressure mechanism · Forming limitation · Thickness distribution

1 Introduction

Internal high-pressure forming is a popular advanced forming technology using high-pressure liquid as the bulging medium and widely used for manufacturing hollow structural parts. It has many advantages compared with traditional T-shaped tube forming technologies such as welding with significant damage to the mechanical performance and increasing the weight of the tube [1]. The products formed by internal high-pressure forming have advantages of better strength, stiffness, and quality of surfaces with lower cost and weight reduction [2–4].

Based on the internal high-pressure forming technology, many researchers proposed different advanced approaches. Trana [5] and Ray [6] carried out complete simulations of the tube hydroforming process. The results, including the branch height and the wall thickness distributions, were in good agreement. Feng et al. [7] used DYNAFORM software to simulate the forming process and studied the forming performance under different loading paths by using the response surface method. Liu et al. [8] analyzed and the relationship between the internal pressure and the clamping speed. The results show that the liquid impact forming has high efficiency and low energy consumption without external pressure. Dai [9] proposed a new inclined angle down material hydroforming method with three different degrees and obtained better thickness distributions. However, there are still some shortcomings to be improved since they require a complete seal device. The whole experiment needs special equipment and a complex control system.

✉ Zhiren Han
hanren888@163.com

1 Key Laboratory of Fundamental Science for National Defence of Aeronautical Digital Manufacturing Process, College of Aerospace Engineering, Shenyang Aerospace University, Shenyang 110136, China
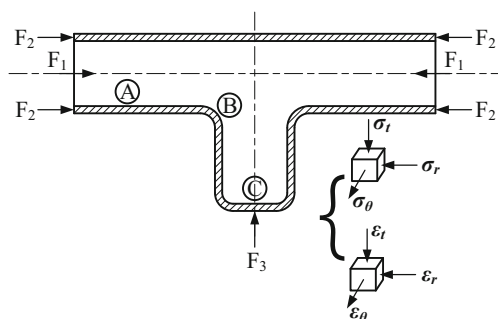
Fig. 1 Principle of T-shaped tube compound bulging forming

To solve the shortcomings mentioned above, the internal high-pressure forming technology using rubber rods as bulging forming medium has been proposed with further advantages [10]. The rubber rods can be quickly restored to their original state and easily taken out from the workpiece, which can be recycled and reused. Besides, bulging the T-shaped tube with a rubber medium can ignore the airtightness of the equipment without the need for a sealing system, and the experiments are simper which can be completed on a general stamping machine. Nosrati et al. [11] studied the tube hydroforming and rubber pad forming and concluded that the better formability of tube will be obtained in the bulging using rubber medium. Koubaa et al. [12] investigated the effect of rubber pads on forming capability compared with hydroforming by using a numerical simulation method. The comparison results show that polyurethane rubber as a flexible medium is recommended to reduce thinning and enhance forming capability. Belhassen et al. [13] investigated the bulging process of aluminum AA1050-H14 sheet metal using a flexible punch with three types of rubber with different hardness. The results show that the polyurethane rubber with hardness of 70 shore A is the most suitable for bulging forming.

In recent years, the compound bulging forming method has been investigated and applied widely. Gao et al. [14] introduced the theory of compound bulging forming based on the tri-branch tubes and verified the feasibility of compound bulging forming in manufacturing tri-branch tube. Wang [15] simulated the compound bulging process and concluded that

using the ramp load patterns could achieve better results. Chen [16, 17] established the finite element model of the T-branch tube compound bulging using a rubber medium and added a rigid punch at the top of the branch tube. After it formed to a certain height, the rigid punch began to apply a balanced backpressure. Zou [18] found that the height of the branch increased first and then decreased with the increase of backpressure time. Therefore, the backpressure is the critical factor that can influence the height of the T-tube branch and the distribution of wall thickness in compound bulging forming. However, the backpressure device is not described in studies. There are two traditional methods of applying backpressure: elastic backpressure devices and rigid backpressure devices [19]. In compound bulging forming, the backpressure is usually provided by the rigid punches fixed in the branch cavity of dies and connected with the hydraulic pressure system. The stiff punches move along the direction of the branch through the control system. However, it is not convenient because of adding experimental costs and processing steps. Also, it is hard to control the time of adding backpressure accurately, which can influence the branch height. Therefore, it is necessary to design a new backpressure mechanism for rubber compound bulging forming.

In this study, aiming at the problems that traditional backpressure device has a complicated structure and is not conducive to accurately adding backpressure, a new position-limited backpressure mechanism made up of the rigid position-limited lever, the flexible backpressure rubber, and the rigid spacer is proposed and designed for the rubber flexible-die compound bulging forming of the T-tube. The effects of three key factors on forming limitations and the wall thickness distributions are investigated: the punch front distance l_1, the reverse height h_1, and the matching relationship between rubber hardness and axial feed. The numerical simulations and experimental research of compound bulging forming processes are carried out, and both results are in good agreement. Through the results, the laws of forming limitation and the wall thickness distributions are analyzed, and the best forming scheme is achieved.
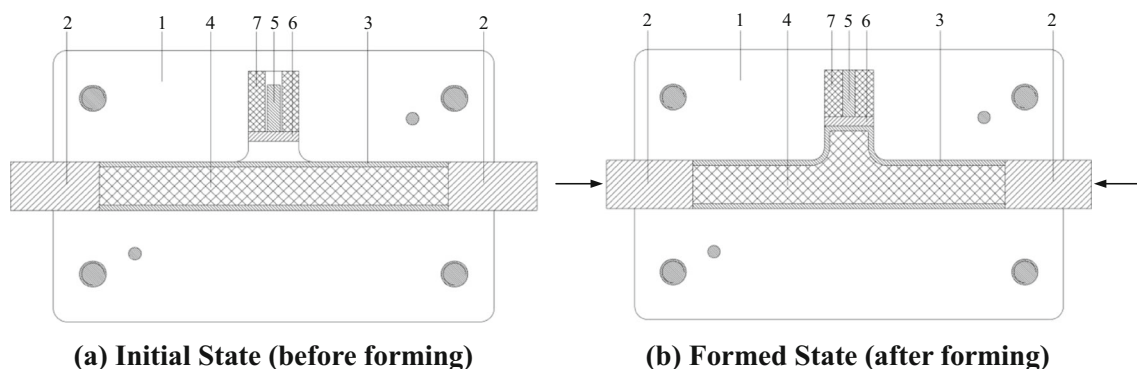

(a) Initial State (before forming)   **(b) Formed State (after forming)**

Fig. 2 Compound bulging forming mechanism. **a** Initial state (before forming). **b** Formed state (after forming)
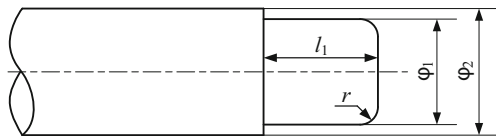
Fig. 3 Schematic diagram of punch

2 Methodology

2.1 Compound bulging forming principle

The T-shaped tube bulging forming can be divided into three zones: (A) guiding zone, (B) transition zone, and (C) expansion zone. The T-shaped tube compound bulging forming mechanical state is shown in Fig. 1 [19, 20].

The compounding bulging mechanical state can be concluded as follows:

(1) The force F_1 acts on the end faces of the rubber rod and makes the rubber rod compressed under the action of axial feed to generate internal force. The internal force will make the tube enter the stage of plastic deformation and form a branch initially.

(2) With the feed of punches increases, the force F_2 acting on the two ends of the tube will make the metal material flow from zone A (guiding zone) into zone C (expansion zone) along zone B (transition zone) to form the branch further, which can alleviate the tube wall thinning caused by the generation of the branch.

(3) The force F_3 represents the backpressure acting on the branch in zone C (expansion zone), which can effectively avoid the rupture at the top of the branch and improve the forming limitation.

Under the effect of "internal force-axial force-longitudinal force" above, the height of the T-shaped tube branch and the wall thickness distributions can be improved.

2.2 Forming processes

The tube compound bulging forming mechanism with polyurethane rubber is shown in Fig. 2 (1, die; 2, axial punches; 3,
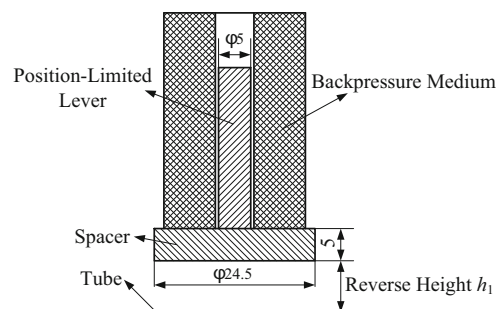

Fig. 4 Schematic diagram of the position-limited backpressure mechanism

Table 1 Material properties of Brass H85

Mechanical Properties	Value
Density/kg·m^{-3}	8750
Young's modulus/MPa	119000
Poisson's Ratio	0.3
Yield strength/MPa	305
Tensile strength/MPa	382
Tangent modulus/MPa	590

tube; 4, polyurethane rubber rod; 5, rigid position-limited lever; 6, rigid spacer; 7, flexible backpressure medium).

The forming processes are described as follows:

(1) Before experiments, tube and die cavity faces are buffed by abrasive paper and smeared with lube to decrease friction. The dies are put on the workbench. The tube, polyurethane rubber rod, and position-limited backpressure mechanism are assembled as shown in Fig. 2, start the hydraulic press machine.

(2) During forming, the front faces of punches contact the polyurethane rubber rod first, and then with the feed of axial punches, the behind faces of punches contact tube, and the tube is compressed along the axial direction. With the action of F_1 and F_2 together, the materials flow to the free space of the die cavity gradually and form the branch.

(3) With the increase of deformation, the top of branch contacts to the position-limited backpressure mechanism, and the backpressure mechanism provides backpressure F_3 to balance the internal force F_1 and the axial force F2 to suppress thinning and avoid rupturing.

(4) Stop feeding when the height of the branch reaches the ideal height, draw back the punches, and open dies to take out the T-tube and finish bulging forming.

2.3 Main influence factors

2.3.1 Punch front distance l_1

The structural parameters of punches are shown in Fig. 3.

The punch front diameter φ_1 is same as the diameter of the rubber rod. Punch outer diameter is same as the outer diameter

Table 2 Theoretical coefficients of polyurethane rubber

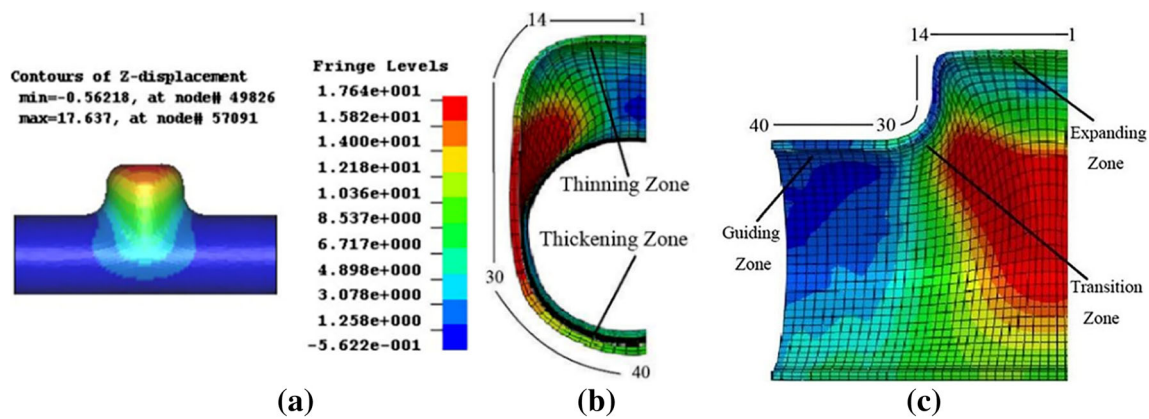| Rubber hardness	C_{10}/MPa	C_{01}/MPa
60HA	0.302	0.076
75HA	0.736	0.184
90HA	2.824	0.706

Fig. 5. **a** Z-displacement cloud Figure, **b** longitudinal cross-section, **c** horizontal cross-section

of tube blank. The punch front surface is chamfered with $r=0.25$mm to prevent the rubber surface from being damaged by punch extrusion. The punch contacts the front face of the rubber rod first, and then during forming, the punches add force to the rubber rod and tube in proper order. The larger l_1 is, the later the bulging zone will be refilled, the pressure acting on the inner cavity of the tube will increase too fast, and the wall thickness will reduce rapidly. The smaller l_1 is, the earlier the bulging zone will be refilled. In the initial period of the experiment, the internal pressure is too small to support the deformation of the tube. Therefore, the punch front distance l_1 is an essential factor, the impact of the punch front distance l_1 on forming results will be analyzed.

2.3.2 Reverse height h_1

The new position-limited backpressure mechanism, including rigid position-limited lever, flexible backpressure medium (polyurethane rubber rod), and rigid spacer, was proposed as shown in Fig. 4.
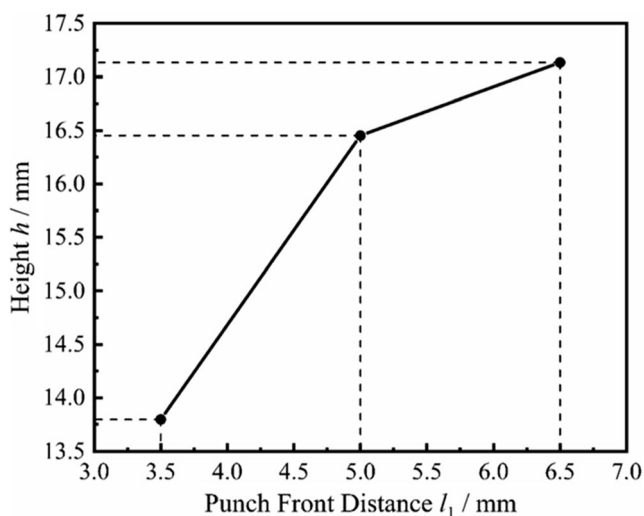

Fig. 6. Height of branch with different punch front distances l_1 in simulation

The rigid position-limited lever is fixed on the center of the rigid spacer, and the flexible backpressure medium is designed as a hollow cylindrical polyurethane rubber rod. The flexible backpressure rubber rod is longer than the rigid position-limited lever, and the inner diameter of the flexible backpressure rubber rod is also bigger than the diameter of rigid position-limited lever. One side of the flexible backpressure rubber rod is fixed with a rigid spacer, and the other side is fixed at the bottom of the branch cavity.

During forming, the tube is acted by the internal force and axial force together for a while before it starts to contact the backpressure mechanism. The reverse height h_1 represents the distance between the tube and the position-limited backpressure mechanism. Thereby it also determines the time when the backpressure is added to the branch.

The backpressure of the new position-limited backpressure mechanism is generated by flexible medium (polyurethane rubber rod) first, the backpressure increases gradually with compression of the flexible medium, and then with the moving of rigid spacer, the rigid spacer contacts rigid position-limited lever finally, and the backpressure maintains unchanged. In this study, the reverse height h_1 is one of the critical factors for the T-tube bulging process, the impact of the reverse height h_1 on forming results will be analyzed.

2.3.3 Matching relationship between rubber hardness and axial feed

The matching relationship between the rubber hardness and feed of axial punches is named as load path. The internal force is generated by the compression of the polyurethane rubber rod, which is related to the hardness of the rubber rod and its properties. As a medium of transferring force, the rubber hardness directly affects the internal pressure acting on the inner wall of the tube. The axial feed of punches makes the rubber rod compressed, which significantly influences the pressure in the tube. Therefore, the matching relationship between the rubber hardness and axial feed (MRRHAF) is another critical factor.

Fig. 7 Wall thickness distributions with different punch front distance l_1 in simulation. **a** Longitudinal cross-section. **b** Horizontal cross-section

(a) Longitudinal Cross-Section

(b) Horizontal Cross-Section
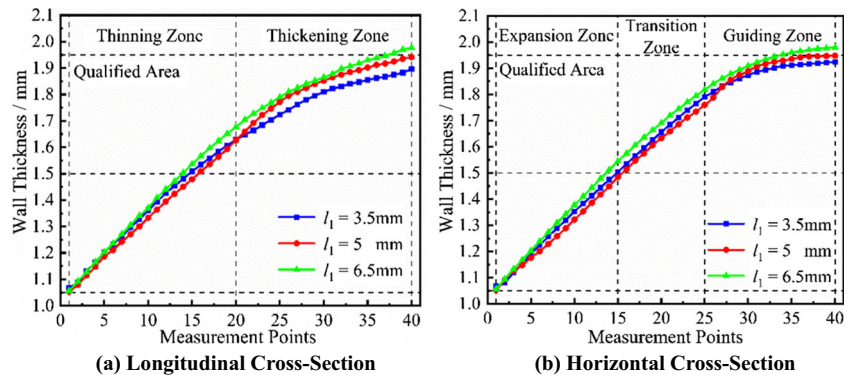
The Mooney-Rivlin model can describe the relationship between the polyurethane rubber hardness and the energy as Eq. (1) [21, 22]. In the theoretical coefficients C_{10} and C_{01} obtained by fitting the stress-strain data, the primary energy density function can be expressed as follows:

$$W_R = \sum_{i,j=0}^{\infty} C_{ij}(I_1-3)^i(I_2-3)^j \tag{1}$$

where I_1 and I_2 represent strain invariants, Eq. (1) can be simplified as:

$$W = C_{10}(I_1-3) + C_{01}(I_2-3) \tag{2}$$

The relationship between principal stress σ and principal elongation ratio λ can be obtained as follows:

$$\sigma = 2\left(\lambda-\frac{1}{\lambda^2}\right)\left(\frac{\partial W}{\partial I_1} + \frac{1}{\lambda}\frac{\partial W}{\partial I_2}\right) \tag{3}$$

where λ=1+ε

Equation (4) will be obtained by combining elongation λ and stress value σ:

$$C_{10} + \frac{1}{\lambda}C_{01} = \frac{\sigma}{2\left(\lambda^2-\frac{1}{\lambda}\right)} \tag{4}$$

Based on the assumption that the wall thickness before and after deformation remains unchanged, the ideal feed of the tube can be estimated as follows [23, 24]:

$$\Delta l = L_0-L_1 = \frac{Dl}{d} + \frac{D^2-d^2}{2d\sin\alpha} - L \tag{5}$$

where L_0 is the original length of the tube, L_1 is the length of tuber after forming, L is the length of tube in forming zone (expansion zone), the length of maximum diameter is $l=L$-(D-d)/tanα, α represents transition fillet, d is inner diameter, and D is the outer diameter of the tube.

The impact of the matching relationship between the rubber hardness and the axial feed (MRRHAF) will be analyzed.

3 Numerical simulation on rubber flexible-die forming of tube

3.1 Finite element modeling

The tube rubber flexible-die forming process was simulated using finite element software ANSYS Workbench with Workbench LS-DYNA module. Before the simulation, the material of the tube was defined as Brass H85, and the material properties of Brass H85 are listed in Table 1.

The polyurethane rubber was selected as the bulging forming medium, and the theoretical Mooney-Rivlin coefficients of polyurethane rubber with three different hardness (60HA, 75HA, and 90HA) are shown in Table 2.

And then, the geometry model was simplified and built, including dies, tube, polyurethane rubber rod, axial punches, and position-limited backpressure mechanism. The original length L_0 of the tube in finite element simulation can be calculated as follows [25]:
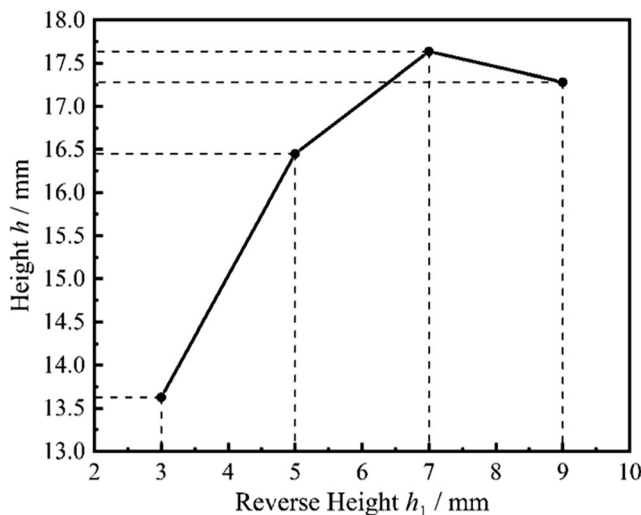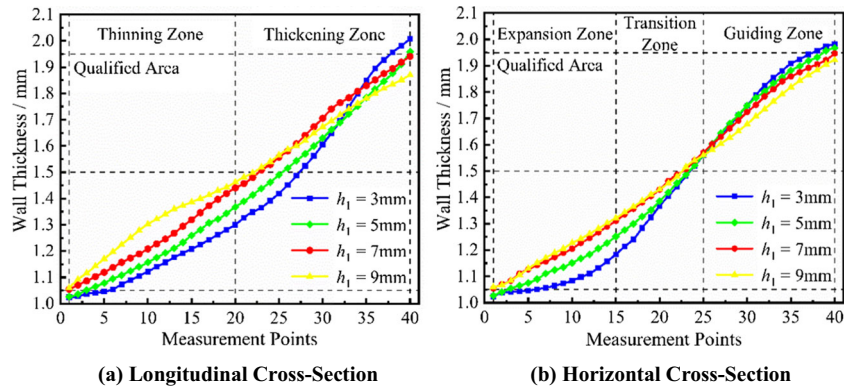

Fig. 8 Height of branch with different reverse height h_1 in simulation

Fig. 9 Wall thickness distributions with different reverse height h_1 in simulation. **a** Longitudinal cross-section. **b** Horizontal cross-section

(a) Longitudinal Cross-Section

(b) Horizontal Cross-Section

$$L_0 = L_t + h - \frac{4(D^2 + Dd + d^2)}{3\pi(D + d)} + \frac{d^2}{2(D + d)} \quad (6)$$

where L_t is the length of the tube at a specific time during forming, h is the branch height, d is the inner diameter, and D is the outer diameter of the tube.

In this study, the outer diameter of tube D is 24mm, and the inner diameter of tube d is 21mm. The original length of tube L_0 is 120mm through initial simulation, and the length of rubber rod l_0 is 118mm, and the diameter d_0 is 20mm. The transition radius of dies is 7mm, and the diameter of the branch and cavity is 24.5mm.

After that, the geometry parts were assigned with corresponding materials. The actual conditions defined the contacts between components, the friction coefficient between the outer face of the tube and the inner face of the die cavity was set as 0.1, and the friction coefficient between the rubber and the inner face of the tube was set as 0.25 according to Coulomb's law of sliding friction. In the aspect of meshing, the rigid bodies such as dies, axial punches, rigid position-limited lever, and rigid spacer can mesh roughly appropriately. The flexible bodies such as the tube, the polyurethane rubber rod, and the flexible backpressure medium should mesh fine.

In the aspect of boundary conditions, the dies were fixed with the limitation of six degrees. The position-limited backpressure mechanism moved only along the parallel direction of the branch, and the axial punches moved only along the horizontal direction of the cavity. According to Eq. (5), the ideal axial feed Δl was calculated as 31.4mm. However, the

actual feed is smaller than the ideal feed and 70–80% of the ideal feed, and the actual feed was about 21.98–25.12mm. Therefore, the feed Δl can be selected as 23mm, 24mm, and 25mm. The loading velocity of axial punches can be enlarged appropriately, and the simulation time was set 0.1s.

3.2 Analysis of finite element simulation results

In the simulation, the deformation cloud figures along the branch direction show the distribution of displacements along the branch. The maximum value of displacement represents the height of the T-shaped tube branch. The T-shaped tube formed can be sliced along the longitudinal cross-section and the horizontal cross-section, and forty points can be defined and obtained along the outer wall from top to bottom of the T-tube. Therefore, the branch height can be obtained from the Z-displacement figures, and the wall thickness distribution along the longitudinal cross-section and the horizontal cross-section can be measured as shown in Fig. 5.

The allowable wall thickness thickening rate and thinning rate are no more than 30%. The maximum thinning rate and the maximum thickening rate can be calculated as follows [26, 27]:

$$\begin{cases} \delta_1 = \frac{t - t_{min}}{t} \times 100\% = \left(1 - \frac{t_{min}}{t}\right) \times 100\% \\ \delta_2 = \frac{t_{max} - t}{t} \times 100\% = \left(\frac{t_{max}}{t} - 1\right) \times 100\% \end{cases} \quad (7)$$

where t represents the wall thickness, t_{min} is the minimum wall thickness, and t_{max} is the maximum wall thickness.

Fig. 10 Maximum principal stress cloud figures of T-shaped tubes with ruptures. **a** 90 HA Δl=23mm. **b** 90HA Δl=24mm
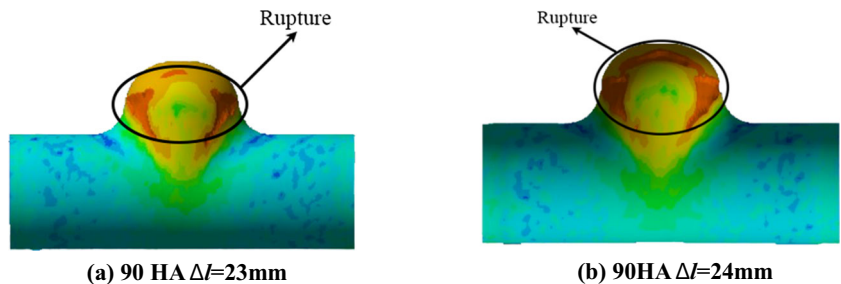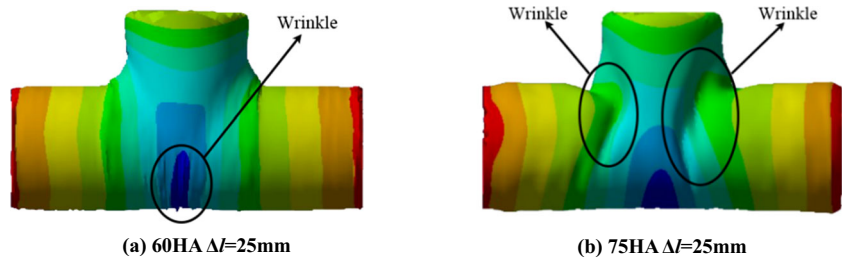

(a) 90 HA Δl=23mm

(b) 90HA Δl=24mm

Fig. 11 T-shaped tubes with wrinkles in simulation. **a** 60HA Δl=25mm. **b** 75HA Δl=25mm

(a) 60HA Δl=25mm   (b) 75HA Δl=25mm

3.2.1 Effect of punch front distance l_1

The punch front distance l_1 was set as 3.5mm, 5mm, and 6.5mm; the polyurethane rubber rod hardness was selected with 60HA; the feed of axial punches was set Δl=23mm; and the reverse height h_1 was 7mm. The height of branch formed by different punch front distance l_1 can be measured, and the results are shown in Fig. 6.

It can be found from Fig. 6 that when l_1 is 3.5mm, 5mm, and 6.5mm, the branch height h reaches 13.797mm, 16.453mm, and 17.134mm. It can be drawn that the larger punch front distance can make the rubber rod compressed more adequately under the action of axial punches so that the rubber rod can generate sufficient internal pressure, which is better for the height of branch. The height of the T-tube branch formed with l_1 = 5mm and 6.5mm are better than it formed with l_1 = 3.5mm. With the increase of punch front distance l_1, the height of the T-tube branch increases, and the height of the branch reaches the largest when l_1 is 6.5mm.

The wall thickness distributions along the longitudinal cross-section and the horizontal cross-section are shown in Fig. 7.

It can be seen from Fig. 7 that in the longitudinal cross-section, the wall thickness gradually increases from the top to the bottom of the branch. In the horizontal cross-section, the wall thickness increases in expansion and transition zone and hardly changes in the guiding zone. The wall thickness of the tube is equal to requirements when l_1 is 3.5mm and 5mm, which illustrates that larger punch front distance makes branch higher. However, too large punch front distance can cause the supplements of materials untimely during compression of the tube, and there is a risk of thinning and thickening. Combing the branch height shown in Fig. 6, the quality of the T-shaped

tube branch formed is higher when l_1 is 5mm. Therefore, the punch front distance l_1 as 5mm is the best in simulation.

3.2.2 Effect of reverse height h_1

The rubber hardness was 60HA, the feed of axial punch was 23mm, the punch front distance l_1 was 5mm, and the different values of reverse height h_1 were set as 3mm, 5mm, 7mm, and 9mm. The height of the T-tube branch formed by different reverse heights can be obtained and shown in Fig. 8.

According to Fig. 8, it can be found that too small reverse height will make the time short when the backpressure mechanism contacts the top of the branch, which also means adding reverse force to branch too early can cause the forming inadequately, so the height of branch cannot reach the ideal height. However, with the increase of reverse height h_1, the height of the branch increases first and then decreases. Too large reverse height will cause the branch to reach the maximum height before contacting the backpressure mechanism, and the branch height will not increase under the limitation of forming performance. Therefore, the reverse height is not the larger the better. The wall thickness distributions were measured and shown in Fig. 9.

It can be found from Fig. 9 that when the reverse height h_1 is 3mm, the range of wall thickness distribution is the widest, and the thinning rate and thickening rate are more than 30% out of the qualified area. When the reverse height h_1 is 5mm, the maximum wall thickness along the horizontal cross-section is 1.9589mm, which is not satisfied with the requirements of thickening rate. When the reverse height h_1 is 7mm and 9mm, the wall thickness distributes in the qualified area. With the increase of reverse height, the minimum wall thickness increases, and the maximum wall thickness decreases gradually. Therefore, the reasonable reverse height can

Table 3 Results in simulation with different load paths (MRRHAF)

Group	Rubber hardness	Feed Δl/mm	Height h/mm	Thickness (max)/mm	Thickness (min)/mm
(1)	60HA	23	15.4728	1.9328	1.0595
(2)	75HA	23	16.4154	1.9421	1.0486
(4)	60HA	24	16.5446	1.9469	1.0521
(5)	75HA	24	17.4732	1.8613	1.0562
(9)	90HA	25	17.3749	1.9654	1.0253

Fig. 12 Wall thickness distributions with different load paths (MRRHAF) in simulation. **a** Longitudinal cross-section. **b** Horizontal cross-section

(a) Longitudinal Cross-Section   **(b) Horizontal Cross-Section**
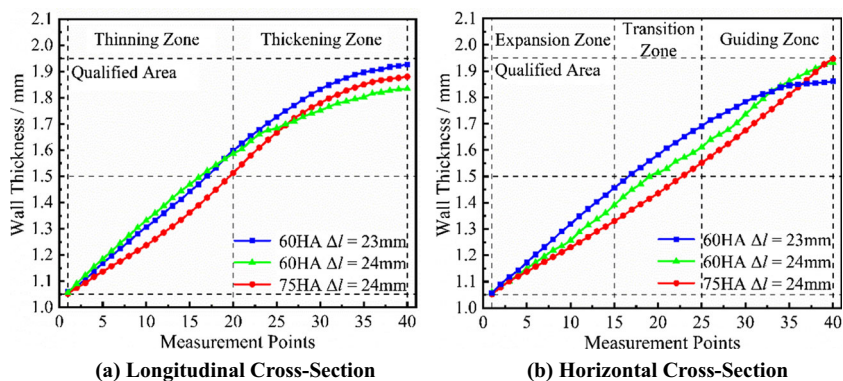
effectively reduce the wall thickness thinning in the top of the tube branch and improve the forming performance with higher forming limitation.

3.2.3 Effect of load path (MRRHAF)

Three different hardness (60HA, 75HA, and 90HA) of polyurethane rubber rod were adopted; and the feed of axial punches Δl were set to 23mm, 24mm, and 25mm; the punch front distance l_1 was 5mm; and the reverse height h_1 was 7mm. There are two main types of failures: wrinkles and ruptures during the internal high-pressure forming of the T-shaped tube.

Ruptures According to the principle of compound bulging shown in Fig. 1, the branch top is under the state of double directional tensile stress and single directional compressive stress. When the branch top cannot withstand the tensile stress caused by the internal pressure, the ruptures usually occur on the top of the branch [28]. In the simulation, the ruptures on the branch top can be estimated through the maximum principal stress cloud figures compared with the tensile strength of the tube [29]. According to the simulation results, when the rubber hardness is 90HA, and the axial feeds are 23mm and 24mm, the ruptures usually occur on the branch top. In the Workbench LS-DYNA module, by using the function of Capped Isosurface, the value of tensile strength can be set in the maximum principal stress cloud figures, and the elements with the larger value of maximum principal

stress than the tensile strength will be deleted; the maximum principal stress cloud figures of T-shaped tube with ruptures are shown in Fig. 10.

Fig. 10 shows the maximum principal stress cloud figures of T-shaped tube with ruptures on the top of branch. When the value of maximum principal stress is bigger than the tensile strength, the elements of the outer surface of the T-shaped tube are deleted. The ruptures usually occur on the top of branch or near the transition zone.

Wrinkles As shown in Fig. 1, with the increase of axial feed, the rubber rod and the tube are compressed under F_1 and F_2. However, when the axial feed is too large and the internal pressure is not enough to match the axial feed of the tube, wrinkles will usually occur in the middle of the main tube. In simulation, in order to estimate the wrinkling, the finite element model of tube was built by using shell element. According to the simulation results of MRRHAF, the wrinkles occur when the axial feed is 25mm and the rubber hardness are 60HA and 75HA as shown in Fig. 11.

Fig. 11 shows the T-shaped tubes with wrinkles in simulation. The wrinkles usually occur at the bottom of the main tube and in the transition zone.

The results without failures of different load paths (MRRHAF) were listed in Table 3.

According to the data, the results of (1), (4) and (5) satisfy the requirements. When the rubber hardness is 75HA and the feed of axial punches Δl is 24mm, the branch reaches the highest. The wall thickness distributions of (1), (4), and (5) were measured as shown in Fig. 12.

It can be found from Fig. 12 that the wall thickness decreases quickly in the thinning zone and the wall thickness increases slowly in the thickening zone along the longitudinal cross-section. Along the horizontal cross-section, the wall thickness increases. When the rubber hardness is 60HA and the axial feed is 23mm, the thickening rate decreases gradually, and when the rubber hardness is 75HA and the feed is 24mm, the thickness changes the most uniformly. Therefore, combing with the branch height, the best matching relationship between rubber hardness and feed is that rubber hardness
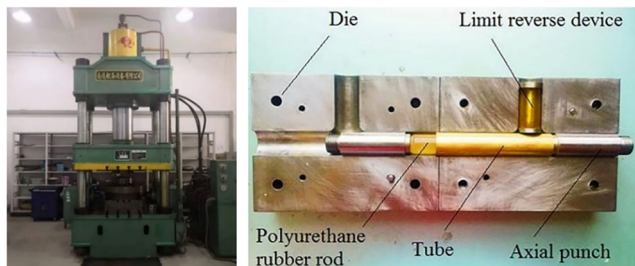

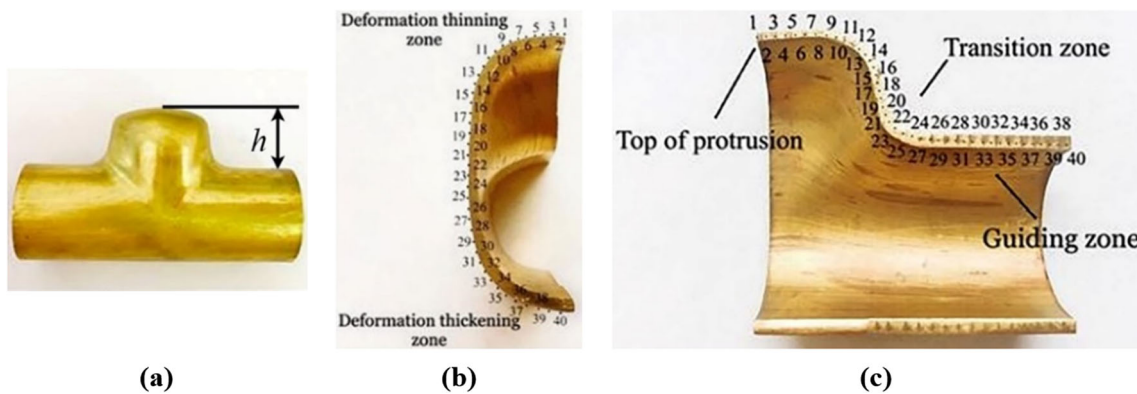**Fig. 13** YQ32-400 hydraulic press and forming device

Fig.14 **a** Height of branch h, **b** longitudinal cross-section, **c** horizontal cross-section

is 75HA and feed of axial punches Δl is 24mm in this simulation.

4 Experimental research on rubber compound bulging forming of tube

4.1 Research equipment and scheme

All experiments are carried out on YQ32-400 hydraulic press. The whole experiment system consists of the hydraulic system and forming device shown in Fig. 13. The forming device consists of dies, axial punches, polyurethane rubber rod, tube, and position-limited backpressure mechanism.

Before the experiment, the polyurethane rubber rod was loaded into the tube. The tube, the polyurethane rubber rod, the punches, and the position-limited backpressure mechanism are installed together in the branch cavity of the dies. The size parameters of the tube, the polyurethane, and the dies are the same as those in simulation.
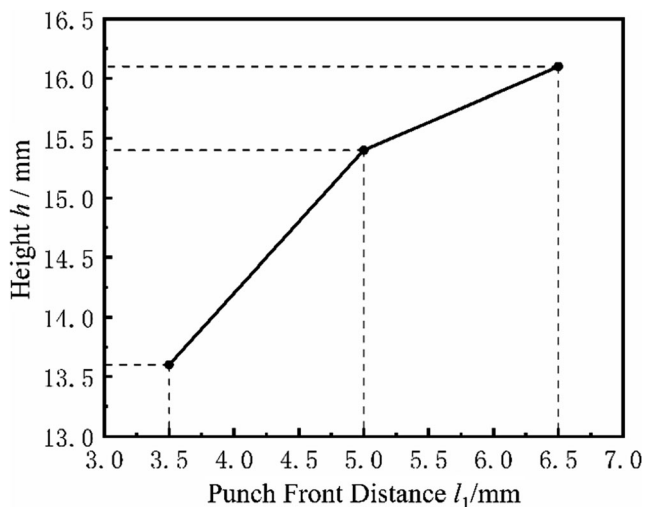

Fig. 15 Height of branch with different punch front distances l_1 in experiments

During forming, the front surfaces of axial punches contact the rubber rod first. With the axial feed punches, the two axial punches synchronously apply force to the rubber rod. The tube and the metal gradually enter the plastic deformation stage and began to expand along with the free space of the cavity. Based on Eq. (5), the actual feed of punches is about 21.98–25.12mm, and the actual feed can be chosen as 23mm, 24mm, and 25mm. In order to control the feed of the tube accurately, the numerical values of the actual feed are marked on the axial punches, which can provide a feasible reference for the experiments. In order to decrease the friction between the tube and the dies and improve the forming performance of tube, the lubricant oil needs to be smeared on the outer wall of the tube uniformly. The aerospace oil was selected as lubricant oil in this experiment because of its good compatibility of materials. When the branch reaches the ideal height, stop feeding and make the punches restore to the initial position, open the dies, and take out the T-shaped tube from the cavity of dies.

After forming, the T-shaped tube needs to be sliced by an electric spark forming machine, and the measurement points were defined along the longitudinal cross-section and the horizontal cross-section. The height of the branch and the wall thickness distributions can be measured as shown in Fig. 14.

4.2 Analysis of experimental results

4.2.1 Effect of punch front distance l_1

The same parameters were applied into the experiments; the height of branch was measured as shown in Fig. 15; when l_1 is 3.5mm, the height of branch h is 13.6mm; when l_1 is 5mm, the height h is 15.4mm; and when l_1 is 6.5mm, the height h is 16.1mm. With the increase of l_1, the height of the T-shaped tube branch increases, and the largest height of the branch reached 16.1mm when l_1 is 6.5mm. The larger with l_1, the better fluidity of the material, which is conducive to feeding the bulging area.

Fig. 16. Wall thickness distributions with different punch front distances l_1 in experiments. **a** Longitudinal cross-section. **b** Horizontal cross-section

(a) Longitudinal Cross-Section

(b) Horizontal Cross-Section
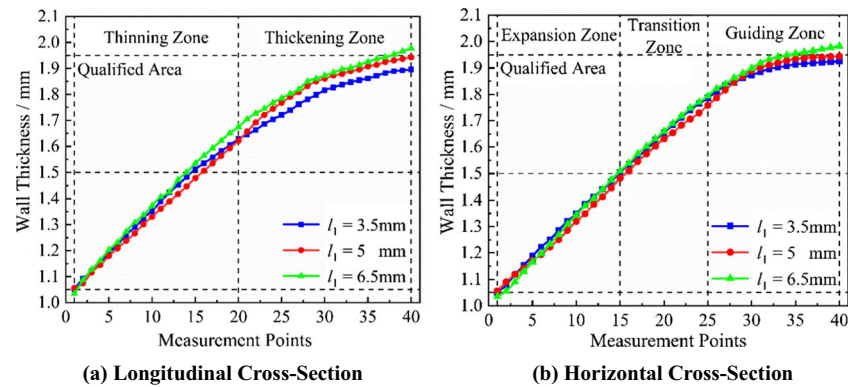
Compared with the results in simulation, when l_1 is 3.5mm, the results in FEM and experiments are in good agreement with relative error of 1.43%. When l_1 is 5mm and 6.5mm, the values of relative error are 6.4% and 6.03%, which are a little bigger than the relative error of 1.43%. The most possible reason is that as the experiments progressed, with the consumption of the lubrication, the friction between the tube and the dies cavity increase, which can limit the metal materials flow resulting in the insufficient forming height.

The wall thickness distributions along the longitudinal and the horizontal cross-section are shown in Fig. 16.

According to Fig. 16, the wall thickness difference is the smallest when l_1 is 3.5mm and the thickness distributions are the most uniform. When l_1 is 5mm, the maximum thickening rate decreases to about 9.6% on the longitudinal cross-section, and the thinning rate significantly decreases to about 1.2% on the horizontal cross-section. When l_1 is 6.5mm, the minimum wall thickness at the top can be obtained from the longitudinal profile as 1.034mm. However, the largest branch height reached 16.1mm; there is a risk of rupture due to the top thinning on the branch tube, which seriously exceeded the qualified area. Both results of simulation and experiments
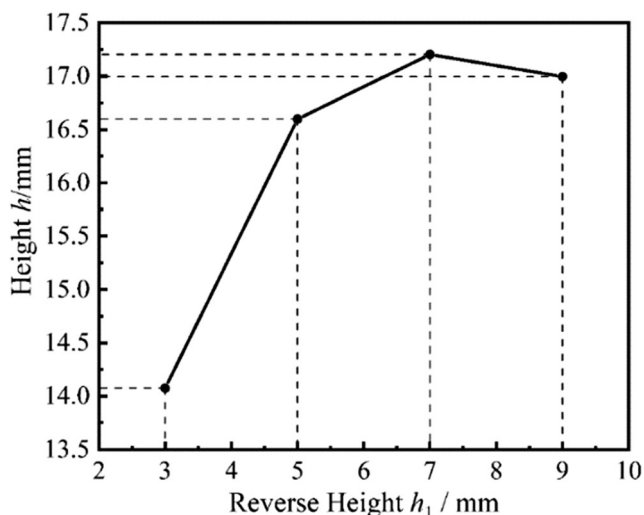
are in good agreement. It can be concluded that when l_1 is 5mm, the height of the T-tube branch can reach the largest in the reasonable range of wall thickness thickening rate and thinning rate, so the punch front distance l_1 of 5mm is the best in experiments.

4.2.2 Effect of reverse height h_1

The impact of reverse height was studied with other corresponding parameters unchanged. The height of the branch formed with different branch heights h_1 can be measured and listed in Fig. 17.

From Fig. 17, it can be seen that when h_1 is 7mm, the maximum height h is formed. The reverse height h_1 determines when the top of the branch tube contacts the position-limited backpressure mechanism. The smaller h_1 will result in a long time of unilateral bulging force on the top of the branch tube, which the thickness becomes thinner and thinner. In contrast, the bigger h_1 will provide a long time of balance force against the bulging to suppress the wall thinning. At the same time, the increase of the branch height is also suppressed. The wall thickness distributions were measured and listed in Fig. 18.

It can be found that both results of simulation and experiments are in good agreement. When h_1 is less than 7mm, the wall thickness of the T-tube blank exceeds the safe area due to not enough balancing force provided. On the other hand, when h_1 is greater than 7mm, the position-limited backpressure mechanism will hinder the metal bulging earlier. Therefore, the wall thickness distributions are in the reasonable range when h_1 is 7mm and 9 mm, and the branch height under the condition of h_1=7mm is larger than h_1=9mm, so the reverse height h_1=7mm is the best in the experiment of T-tube bulging forming.

4.2.3 Effect of load path (MRRHAF)

Three different kinds of rubber hardness (60HA, 75HA, and 90HA) were adopted; the axial feed Δl were set at 23mm,

Fig. 17 Height of branch with different reverse heights h_1 in experiments

Fig. 18 Wall thickness distributions with different reverse heights h_1 in experiments. **a** Longitudinal cross-section. **b** Horizontal cross-section

(a) Longitudinal Cross-Section   **(b) Horizontal Cross-Section**
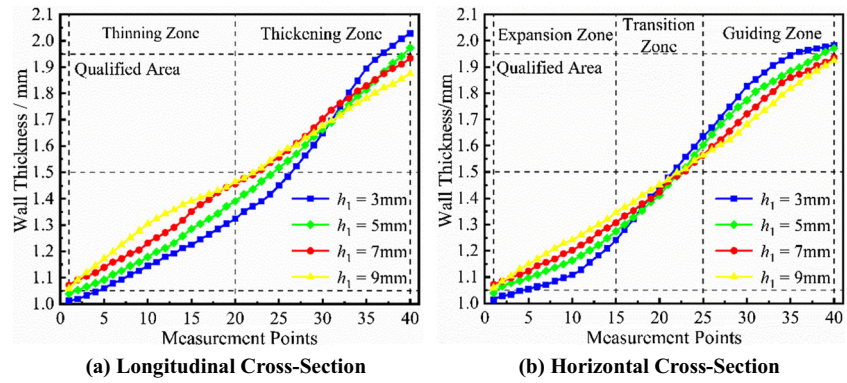
24mm, and 25mm; and the other corresponding process parameters remained unchanged.

In experiments, there are two types of failures, including wrinkles and ruptures, occurred in the research on the effect of load path (MRRHAF) shown in Fig. 19.

Compared with the simulated and experimental results, the failures are ruptures and wrinkles. When the rubber hardness is 90HA and the axial feed is 23mm and 24mm, ruptures occur on the top of the branch. The reason is that the internal pressure generated by the rubber is larger than the tensile strength of materials and the axial feed is too small to make the materials flow into the branch timely. When the axial feed is 25mm and the rubber hardness is 60HA and 75HA, the wrinkles occur at the bottom of the main tube or near the transition. The reason is that the axial feed is too large, the rubber hardness is too small to generate sufficient internal pressure, and the materials accumulate to generate wrinkles.

The branch height and the wall thickness distributions formed by different load paths without failures were measured and listed in Table 4.

According to Table 4, the following conclusions can be obtained from the experiments:

(1) When rubber hardness is 60HA and Δl is 23mm, the branch height is only 15.1mm, which is a little hard to process further.
(2) When rubber hardness is 75HA and Δl is 23mm, the quality of branch formed is better than before without apparent failures, and the surface quality of the T-shaped tube satisfies the forming requirements to be adopted.
(3) When rubber hardness is 90HA and Δl is 23mm, the wall thickness thinning rate on the top of the branch is too large. The top of the branch ruptured because of the hardness of rubber too large, so it is unqualified.
(4) When rubber hardness is 60HA and Δl is 24mm, the T-shaped tube satisfies the bulging forming requirements without failure, and the height of the branch is 16.1mm.
(5) When rubber hardness is 75HA and Δl is 24mm, the quality of the branch satisfies the forming requirements, and the height of the branch reaches 16.9mm.

Fig. 19 Photograph of T-shaped tube with typical failures in experiments. **a** 90HA Δl=23mm, **b** 90HA Δl=24mm, **c** 60HA Δl=25mm, **c** 60HA Δl=25mm, and **d** 75HA Δl=25mm
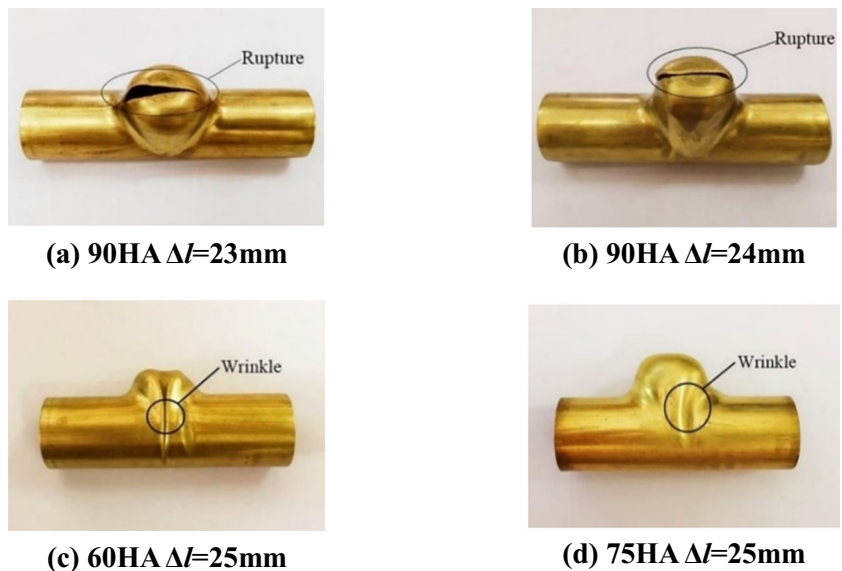

(a) 90HA Δl=23mm   **(b) 90HA Δl=24mm**

(c) 60HA Δl=25mm   **(d) 75HA Δl=25mm**

Group	Rubber hardness	Feed Δl/mm	Height h/mm	Thickness (max)/mm	Thickness (min)/mm
1	60HA	23	15.1	1.932	1.056
2	75HA	23	15.8	1.938	1.042
4	60HA	24	16.1	1.934	1.053
5	75HA	24	16.9	1.943	1.059
9	90HA	25	17.5	1.974	1.015

Table 4 Experiments results without failures of load path (MRRHAF)

(6) When rubber hardness is 90HA and Δl is 24mm, the top of the branch also ruptured, but it is a little better than the forming result (3).

(7) When rubber hardness is 60HA and Δl is 25mm, it can be seen that because the feed is too large, the materials of the tube accumulate seriously to wrinkle, which damaged the rubber rod in the tube.

(8) When rubber hardness is 75HA and Δl is 25mm, the tube also wrinkled, but with the increase of hardness of rubber rod, the wrinkle condition improved better than before; the rubber rod can be taken out from the tube easier than before.

(9) When rubber hardness is 90HA and Δl is 25mm, the branch height reached 17.5mm, which is the largest of nine experiments without failure.

According to the requirements of the wall thickness thickening rate and thinning rate, there are three experiments ((1), (4), and (5)) that satisfy the forming requirements. The wall thickness distributions of (1), (4), and (5) were shown in Fig. 20.

Fig. 20 shows the wall thickness distribution of the three conditions; the working conditions (1), (4), and (5) conform to the safety and qualified area; under the premise of meeting the production conditions, the workpiece with the highest branch height is conducive to subsequent machining; the working condition (5) with the branch height of 16.9mm is considered the best result in experiments. The relationship among the

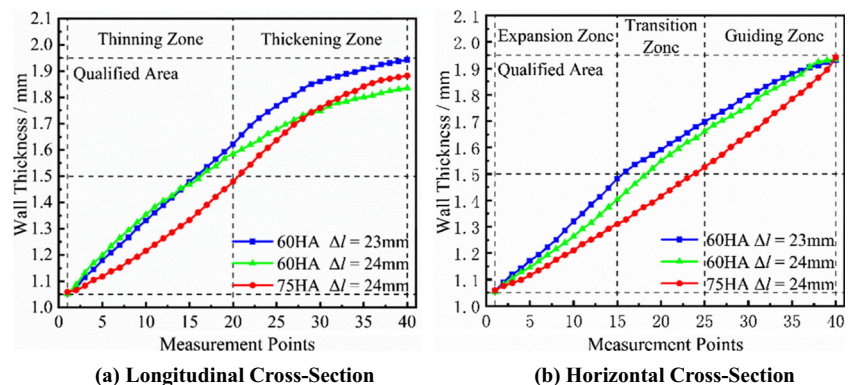rubber hardness, the axial feed, and the height of branch can be shown in Fig. 21.

When rubber hardness is fixed at 90HA, too small feed cannot reach the strength of material compensation, so that the pressure inside the tube increases too fast and the branch ruptures due to insufficient material compensation as shown in Fig. 19a and b. When rubber hardness is fixed at 60HA and 75HA, excessive feed is not conducive to material flow and accumulates at the transition fillet; buckling and wrinkling occur to it which both affect subsequent use as shown in Fig. 19c and d. When axial feed is fixed, the greater rubber hardness and force push the metal to transfer into the branch tube with the increase of rubber hardness, more and more materials are demanded to increase the branch. However, not enough metal is supplemented into the branch tube due to the greater friction resistance. The thinnest part of the tube wall becomes thinner and more uneven and even breaks.

Therefore, compared with the results in simulation, only when the feed is matched with the rubber hardness can the wall thickness be evenly distributed. In this experiment, the best matching relationship of load path is that rubber hardness is 75HA and feed Δl is 24mm.

5 Discussions and conclusions

The numerical simulations and experimental research of rubber flexible-die compound bulging forming with a new

Fig. 20 Wall thickness distributions with different load paths (MRRHAF) in experiments. a Longitudinal cross-section. b Horizontal cross-section

(a) Longitudinal Cross-Section
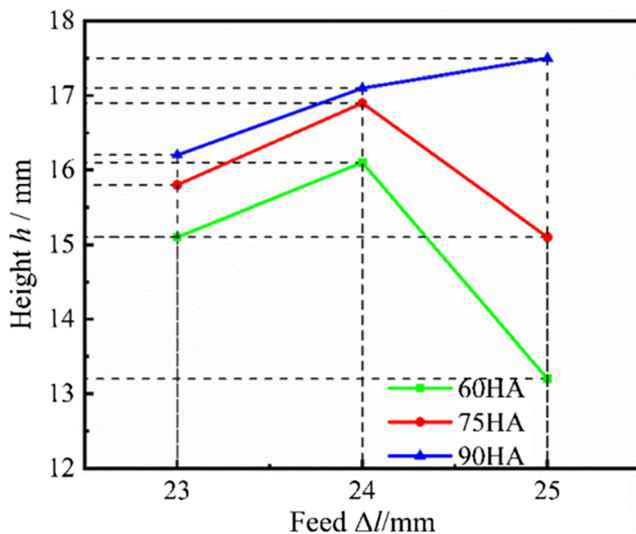
(b) Horizontal Cross-Section

Fig. 21 Relationship among the rubber hardness, the axial feed, and the branch height

position-limited backpressure mechanism were conducted. The effects of three key factors on the forming limitation are investigated, and the thickness distributions along longitudinal and horizontal cross-section are examined in this study. The main conclusions are as follows:

(1) The new position-limited backpressure mechanism is convenient for the experiments because of simple structures, which effectively improves the forming limitation and the wall thickness distributions.

(2) The results of the forming limitation and the wall thickness distributions in the numerical simulations and experiments are in good agreement.

(3) The height of the branch increases with the increase of punch front distance l_1, and the difference of wall thickness increases gradually. With the increase of reverse height h_1, the height of the branch increases first and then decreases, and the difference of wall thickness increases. When the rubber hardness is fixed, the difference of wall thickness increases with the increase of the axial feed. When the axial feed is fixed, the height of the branch increases with the increase of the rubber hardness.

(4) The failures include ruptures and wrinkles in this study. The ruptures usually occur on the branch top because of too large internal pressure. In contrast, the wrinkles usually occur at the middle of the main tube because of excessive axial feed with relatively small rubber hardness. Therefore, the best matching relationship between the rubber hardness and axial feed can avoid failures.

In conclusion, when the punch front distance l_1 is 5mm, the reverse height h_1 is 7mm, rubber hardness is 75HA, and the axial feed Δl is 24mm, the T-shaped tube branch reaches the maximum forming limitation with the most uniform wall thickness.

Declarations

Ethics approval The work was original research that has not been published previously, and not under consideration for publication elsewhere, in whole or in part.

Consent to participate The authors all approved to participate.

Consent for publication It is approved by all authors for publication

Conflict of interest The authors declare no competing interests.

Additional declarations for articles in life science journals that report the results of studies involving humans and/or animals Not applicable

References

1. Vakili-Tahami F, Majnoun P, Ziaei-Asl A (2019) Controlling the in-service welding parameters for T-shape steel pipes using neural network. Int J Press Vessel Pip 175:103937
2. Dong GJ, Bi J, Du B, Chen XH, Zhao CC (2017) Research on AA6061 tubular components prepared by combined technology of heat treatment and internal high pressure forming. J Mater Process Technol 242:126–138
3. Lang LH, Yuan SJ, Wang ZR, Wang XS, Danckert J, Nielsen KB (2004) Experimental and numerical investigation into useful wrinkling during aluminium alloy internal high-pressure forming. Proc Inst Mech Eng B J Eng Manuf 218(1):43–49
4. Yuan SJ, Liu G (2014) 3.04-Tube Hydroforming (Internal High-Pressure Forming). In: Comprehensive Materials Processing, Hashmi S, Batalha GF, Van Tyne CJ, Yibas B, Eds. Oxford: Elsevier, pp 55–80
5. Trana K (2002) Finite element simulation of the tube hydroforming process-bending performing and hydroforming. J Mater Process Technol 127(3):401–408
6. Ray P, Mac Donald BJ (2005) Experimental study and finite element analysis of simple X- and T-branch tube hydroforming processes. Int J Mech Sci 47:1498–1518
7. Feng YY, Zhang HG, Luo ZA, Wu QL (2019) Loading path optimization of T tube in hydroforming process using response surface method. Int J Adv Manuf Technol 101:1979–1995
8. Liu J, Yao X, Li Y, Liang H, Yang L (2019) Investigation of the generation mechanism of the internal pressure of metal thin-walled tubes based on liquid impact forming. Int J Adv Manuf Technol 105:3427–3436

9. Dai LF (2018) Study on the influence factors of Hydroforming of 5A02 aluminum alloy Reducer Tee. Nanchang Hangkong University

10. Ramezani M, Ripin ZM (2012) Tube bulging using rubber rods. In: Rubber-Pad Forming Processes: Technology and Applicantions, Woohead Publishing, pp 229–256

11. Nosrati HG, Gerdooei M, Naghibi MF (2016) Experimental and numerical study on formability in tube bulging: a comparison between hydroforming and rubber pad forming. Mater Manuf Process 32(12):1353–1359

12. Koubaa S, Belhassen L, Wali M, Dammak F (2017) Numerical investigation of the forming capability of bulge process by using rubber as a forming medium. Int J Adv Manuf Technol 92(5-8):1839–1848

13. Belhassen L, Koubaa S, Wail M, Dammak F (2019) Experimental and numerical investigation of flexible bulging process of aluminum aa1050-h14 sheet metal with soft tools. Int J Adv Manuf Technol 103(9-12):4837–4846

14. Gao HF, Zhao W, Sun AX, Wang M (2003) Study on compound forming of bulging and extrusion of tri-branch tube. Hot Working Technology (6):19–20+64

15. Wang HF (2004) Forming study and process control of the multi-tube's hydroforming. Northwestern Polytechnical University

16. Chen ZZ, Liu B (2011) Simulation of bulge forming process for three-way tube using rubber medium. J Huaqiao Univ (Natural Science) 32:485–491

17. Chen ZZ, Liu B (2011) Simulation of Compound bulging process for T-branch tubes using rubber medium. Adv Mater Res 228-229:88–95

18. Zou QS, Liu B (2013) Influence of mold structure parameters on T-shapes tubes by compound bulging using rubber medium. J Huaqiao Univ (Natural Science) 34:121–125

19. Chen ZZ (2011) Research on compound bulging technology of T-branch tube based on elastic medium. Huaqiao University

20. Wang Y, Nielsen KB, Lang L, Endelt B (2018) Investigation into bulging-pressing compound forming for sheet metal parts with very small radii [J]. Int J Adv Manuf Technol 95:445–457

21. Kim B, Lee SB, Lee J, Cho S, Park H, Park YSH (2012) A comparison among Neo-Hookean model, Mooney-Rivlin model, and Ogden model for chloroprene rubber [J]. Int J Precis Eng Manuf 13(5):759–764

22. Zhang L, Li ZH, Ma XQ (2018) Study on parameter characteristics of rubber Mooney-Rivlin model. Noise Vib Control 38:427–430

23. Liu G, Xie WC, Yuan SJ, Yao JQ, Miao QB (2004) Internal high pressure forming of hollow part with a big section difference. J Mater Sci Technol 12(4):398–401

24. Zhu SJ, Li J, Lin XK, Chang X, Su HD, Wu L (2018) Simulation and optimization on hydroforming of T-shape tube based on orthogonal experiment. Forging & Stamping Technology 43(9):75–82

25. Li XM, Xia JQ, Hu GA (2002) Technology analysis and forming force calculation of compound forming of solid three-way tube. China Metalforming Equipment & Manufacturing Technology 4:37–38

26. Yang ZZ, Wang GF, Liu YL, Huang L, Nie XH, Xu Y, Zhao JL (2019) Correlation between processing technology and cross-sectional distortion of small-radius hot-bending. Oil & Gas Storage and Transportation 38(03):338–344

27. Xu XB, Guan Q (2010) Numerical simulation of wall thickness change in tube bending. Forging & Stamping Technology 35(06):133–136

28. Peng JY, Luo DG, Teng BG, Liu G (2017) Analysis on wrinkling and cracking initiation in hydroforming thin-walled Y-shaped tubes. Mater Sci Technol 25(04):11–16

29. Zhai JB, Yu XH, Zhai NZ (2007) Comparison of T-tube compound bulging and axial-compressive bulging processes. China Metalforming Equipment & Manufacturing Technology 2:82–86